8-2022

Investigations into Flange Surface Friction Effects on Shear Stud Load Transfer in Composite Bridge Girders

Callie Clark
University of Arkansas, Fayetteville

Investigations into Flange Surface Friction Effects on Shear Stud Load Transfer in Composite Bridge Girders

A thesis submitted in partial fulfillment
of the requirements for the degree of
Master of Science in Civil Engineering

by

Callie Clark
LeTourneau University
Bachelor of Science in Engineering – Civil Concentration, 2020

August 2022
University of Arkansas

This thesis is approved for recommendation to the Graduate Council.

_____
Gary S. Prinz, Ph.D.
Thesis Director

_____
W. Micah Hale, Ph.D.
Committee Member

_____
Cameron Murray, Ph.D.
Committee Member

Abstract

Composite bridge behavior is commonly achieved through headed shear studs welded to the steel girder flange and embedded in the concrete deck. Current AASHTO provisions for estimating demands on shear studs during service-level loading consider only bearing load transfer, neglecting adhesion bonding and friction load transfer between the concrete deck and girder flange. Quantifying alternative load transfer mechanisms across the steel-concrete interface may result in improved steel bridge economy by reducing the number of studs required in a composite girder design. This study investigates the effects of flange surface friction (considering various coatings) on resulting stud demands using both experimental testing and analytical modeling. In this study, inorganic zinc primer and cleaned mill-scale surface conditions are considered in analytical simulations, and inorganic zinc primer coatings are considered in double-sided pushout experiments to quantify flange surface coating effects. Thin foil pressure gauges are used to measure stud demands while controlled normal forces are applied to each slab to allow controlled changes in flange friction force during testing. A total of nine experimental tests are conducted. The analytical study involves 32 finite element simulations of pushout geometries having normal forces of 0k, 5k, 10k, 25k, and shear forces of 10k, 15k, 20k, and 25k. Results from both experiments and analyses indicate that moderate increases in applied normal force (10k) result in friction load transfer that reduce stud demands by 86.6% on average. Applied normal forces of 6k resulted in 74% reduction in stud demands when compared to tests having no applied normal force.

Table of Contents

List of Tables

List of Figures

1. Introduction

Composite bridges are commonly constructed by creating a mechanism for load transfer between the cast-in-place concrete deck and steel girders using headed shear studs. Shear studs welded to the girder flange and embedded within the concrete slab provide load transfer through a mechanical interlock (bearing between the steel stud and concrete deck). Additional load transfer mechanisms that may contribute to composite behavior include adhesion between the cast-in-place concrete and steel flange, and friction shear transfer at the steel flange-and concrete slab interface; however, these additional mechanisms are not considered in design. Figure 1 shows studs welded to the top flange of a steel girder prior to placement of the concrete deck.

Figure 1 - Shear studs on a composite bridge prior to concrete pour

Current AASHTO Bridge Design Specification do not currently account for friction as a load transfer mechanisms at the steel-concrete interface (AASHTO 2020). Instead, current code equations assume all load transfer is carried through bearing between the concrete slab and steel studs. While this approach may be reasonable for strength limit-state design considerations, considering friction effects in service-level fatigue loading calculations (which often govern stud pitch design) may result in improved design economy and reduce the number of required shear

studs. In order for such an approach to be implemented, quantification of flange surface friction effects on stud demands is needed.

Existing literature on shear stud performance can be categorized into either stud demand or capacity investigations, with further categorizations investigating fatigue behavior or strength behavior. Figure 2 below shows a general classification of existing stud investigations present in the literature, with separations between analytical and experimental investigations. As an example, studies completed by Slutter and Fisher (Slutter & Fisher, 1966) fit into the experimental stud demand and capacity strength focus category, while other studies performed by Ovuoba and Prinz (2018) and Hillhouse and Prinz (2020) fit into the experimental and analytical fatigue focus for both stud demand and stud capacity investigations. The following paragraphs provide a synthesis of relevant literature reviewing stud demand and capacity investigations.

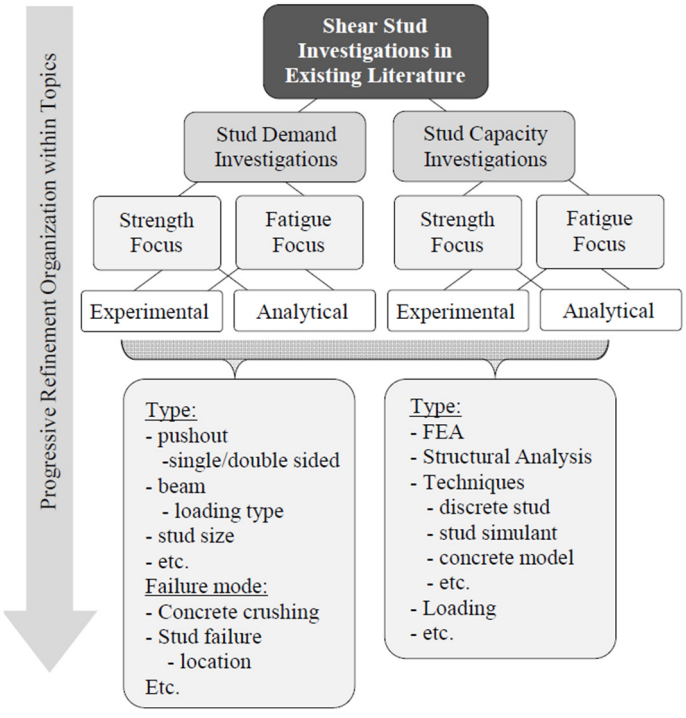

Figure 2 – Literature Categorization

Studies completed in the 1960's by Slutter and Fisher investigated shear stud capacities through high-cycle fatigue testing (Slutter & Fisher, 1966). The American Association of State Highway and Transportation Officials (AASHTO) currently use data from the Slutter and Fisher findings to estimate the fatigue capacity of headed studs, which often governs the number of studs required in a composite bridge design (AASHTO 2020). The Slutter and Fisher equations are solely fatigue results which used greased flanges to reduce friction transfer effects and did not consider other factors such as adhesion, and shrinkage.

Other previous stud investigations include more recent fatigue behavior experiments and the effects of stud clustering and flange surface friction. In Hillhouse and Prinz (2020), flange surface friction effects on resulting stud demands were investigated in composite beam tests loaded in 3-point bending. Comparing stud demands from decks cast in contact with steel flange (cleaned mill-scale surface) and decks separated from the steel flange by Teflon sheets, Hillhouse and Prinz (2020) determined that friction plays a significant role in reducing stud demands. Hillhouse and Prinz (2020) suggest a friction modification coefficient for estimating stud demands to be 0.5 for Class A shear studs or better and 1.0 for all other flange friction conditions; however, only cleaned mill-scale flange surfaces were considered in the experiments. Friction effects from other commonly used flange surface coatings were not considered. Other work by (Luo et al., 2016) (adopted by the PCI Committee) suggests a friction coefficient of 0.4 for contact interaction between a cast in place concrete slab and steel beam flange.

One study compared the required number of shear studs from AASHTO, the Eurocode, the Japanese Standard, and the British Standard (Lee et al., 2010). The findings concluded that each AASHTO fatigue load design case required at least 2-3 times the number of shear studs (Lee et al., 2010).

Fatigue failure is a concern in shear stud connection design. Fatigue failure begins at shear studs near the ends of a member due to higher stresses at the ends of the members under consideration (Sjaarda et al., 2017). This is not consistent with current design assumptions of full composite interaction (Sjaarda et al., 2017). Fatigue failure usually occurs by exhibiting cracks in the base metal (steel girder flange) in the heat-affected zone (HAZ) of the weld (Sjaarda et al., 2017). "The design rules for fatigue of steel structures assume that the static resistance remains intact until the fatigue limit is reached (Veljkovic &Johansson, 2006). Current fatigue design provisions are based on Slutter and Fisher's research conducted on 44 push-test specimen tests in the 1960's (Lee et al., 2010). Slutter and Fisher did not measure the friction effects in their work.

There are three types of connection properties that exist at the flange and concrete interface. The connection types are mechanical bearing, adhesive bond, and friction bond. Mechanical behavior is included in AASHTO provision designs. The bearing behavior of the shear studs is good in large deformation and high strain-rate loading (Huo et al., 2018). This mechanical interlock behavior of the studs is present under any shear load and truck load. The adhesion layer behavior between the concrete deck and steel girder flange is ignored in fatigue design. Numerical analysis methods usually do not consider frictional and bond stresses at the steel concrete interface (Lin et al., 2020). The adhesion layer is present up to a shear limit. After the adhesion layer shear limit has been exceeded, only the friction behavior between the steel girder flanges and concrete deck and mechanical bearing behavior of the studs remain. The adhesion should vary between types of steel treatments used. Friction at the concrete-steel interface is of interest because friction is not accounted for in current AASHTO standards. Friction is complex and is the main reason for inaccurate stress-range calculations (Sjaarda et al., 2017). The AASHTO shear stud design curve has not changed since the 1960's, is very conservative

compared to other countries, and should be updated to accommodate new friction research (Sjaarda et al., 2017). Most of the longitudinal shear stress is transferred through friction bonding at low loads (Lin et al., 2020). One study suggests that the friction behavior depends on the concrete normal compressive force (Xia et al., 2019). Like the adhesion bond, the friction bond should also vary among types of steel treatments used.

Several studies have focused on reducing the number of shear studs in composite bridges. Most study conclusions acknowledge that the friction between the shear stud and concrete is not accounted for. The studies do not account for friction in their experimental work, but they do suggest factors that affect friction behavior. Such examples suggest that the slip behavior of shear studs is governed by the global behavior of the steel beam in the composite bridge (Gattesco et al., 1997). One study suggested that the failure at the concrete and stud interface is not due to a poor friction connection, but the concrete cracking before the friction connection fails (Berthet 2011). This would be a case of the adhesion layer breaking under the shear limit for adhesion. If both the adhesion layer and the friction bonds were better understood, it would be possible to reduce the number of studs in a composite bridge due to the added shear resistance from the adhesion layer and the friction bonds.

One study proposed reducing the number of shear studs in composite bridges by installing large diameter studs (Kakish et al., 1999). Their focus was to reduce stud costs, reduce steel congestion, and reduce construction workers time installing shear studs. They did not consider trying to reduce the number of studs due for fatigue loading. The final suggestion was to use a larger shear stud with a diameter of 1 and ¼ inches rather than 7/8 inches. This way, they could design a bridge with half the number of shear studs, but not decrease the shear stud/concrete

interface area. Although this study did not account for flange friction, it suggested reasons to reduce the amount of studs in a bridge design.

Xu et al. (2018) stated that fatigue behavior is affected by load pattern, amount and clustering of shear studs, and material properties. This study also found that arranging shear studs in a group lowered the fatigue life of the push-test specimens causing slip and creep failure (Xu et al., 2018). Fatigue damage was shown to occur at the root of the shear stud in the surrounding concrete, adjacent to the flange surface. The Xu et al. study did not account for flange friction in their work, but their work furthered the understanding of fatigue behavior. Recent research predicted the number of cycles until fatigue failure of critical studs was 260,000 cycles (Sjaarda et al., 2017).

Concrete strength affects the bearing capacity of the shear studs in a push test. The concrete strength is less of an issue in bearing under low-cycle fatigue tests. Fatigue loads are much lower than stud bearing loads (Xue et al., 2008). The response curves of static shear load/slip relationships exhibit three stages; the elastic stage, the plastic stage, and the descending stage (Huo et al., 2018). The study conducted by Slutter and Fisher in 1966 exhibited stud reaction forces that were approximate to the applied shear force (Lee et al., 2010).

This study investigates the effects of flange surface friction (considering various coatings) on resulting stud demands using both experimental testing and analytical modeling. In this study, inorganic zinc primer and cleaned mill-scale surface conditions are considered in analytical simulations, and inorganic zinc primer coatings are considered in double-sided pushout experiments to quantify flange surface coating effects.

The method of quantifying the effects of flange friction and adhesion requires tracing the load path from the shear force in a bridge to the resultant force acting on the stud embedded in

the concrete deck. One way of achieving a load path is to use pushout specimen geometry design from the Eurocode. Pushout specimens are small composite bridge sections with an added concrete slab to minimize eccentricities under axial loading. A pushout specimen allows for axial loading on the bridge girder (shear force) as well as normal force loading on the concrete slabs. An example pushout specimen is shown in Figure 3.

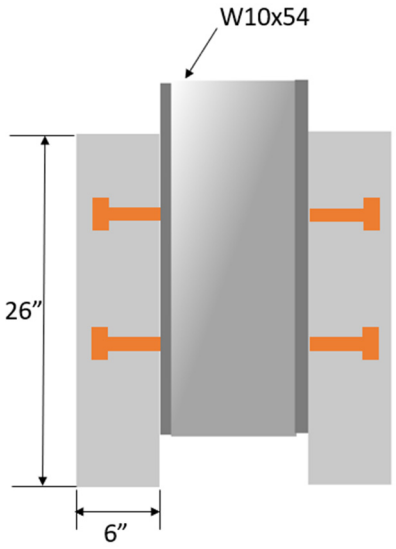

Figure 3 - Pushout specimen diagram

The friction loads are increased under increased normal forces and by increased friction coefficients at the flange-concrete interface. Inorganic zinc (IOZ) steel primer has a higher surface friction coefficient than cleaned mill-scale steel. IOZ primer is common in composite bridge design and was selected to compare friction force results to cleaned mill-scale friction force results. The purpose of this study is to compare the friction force effects of normal forces under different shear load cycles.

2. Experimental Setup and Specimen Fabrication

To experimentally investigate adhesion and friction effects in composite girders, one double-sided pushout specimen was constructed and coated in an inorganic zinc (IOZ) primer prior to

concrete casting. An IOZ primer was chosen for this experimental study because such primers are commonly applied to steel girders prior to deck casting and may affect the friction transfer mechanisms at the interface. The double-sided pushout specimen was fabricated with each slab oriented horizontally as would be constructed in the field. Figure 4 shows the specimen geometry, slab rebar detail, and Figure 5 shows the specimen fabrication setup prior to casting. The chosen double-sided geometry (having a concrete slab on both sides of the girder) reduces the potential for eccentric loading on the shear studs.

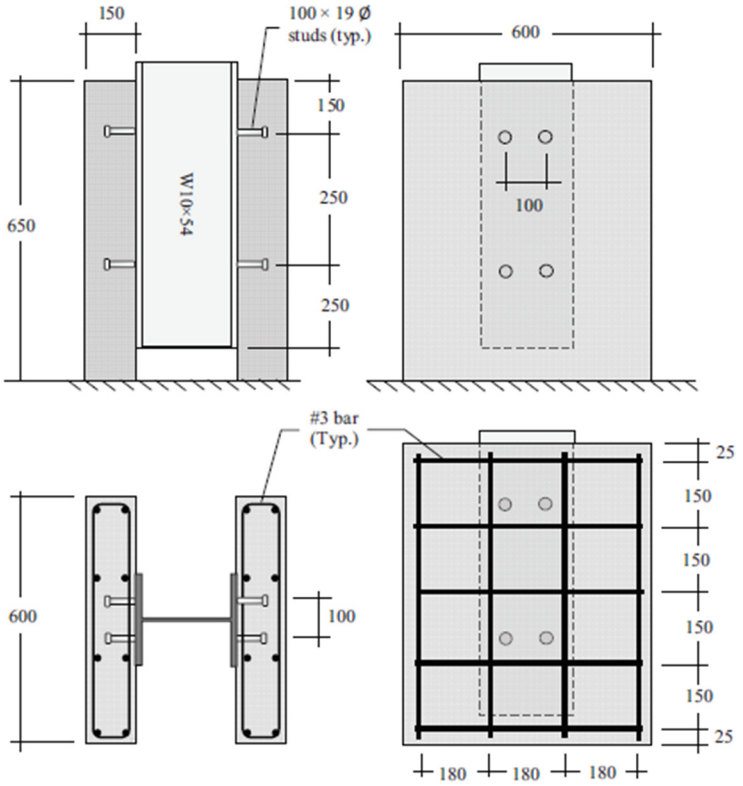

Figure 4 - Pushout specimen geometry, also used by (Ovuoba & Prinz, 2016)

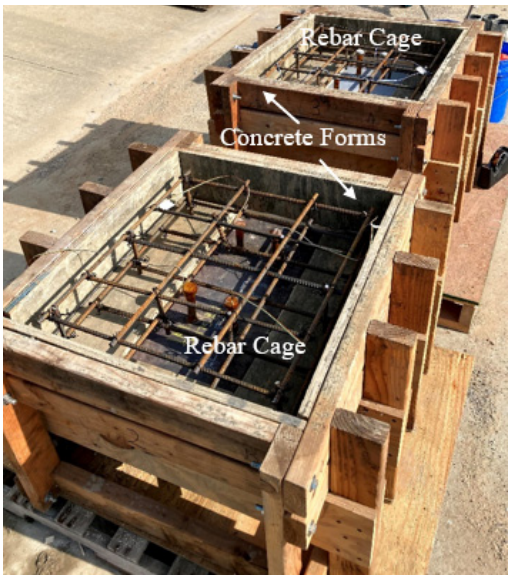

Figure 5 - Concrete forms ready for concrete pour

Concrete material properties were intended to represent a typical Arkansas Department of Transportation (ArDOT) bridge deck mix. Table 1 presents the mix design considered for the specimen slabs and Table 2 presents the resulting average 28-day compressive strengths from three cylinders.

Table 1 - Concrete batch info – 0.211 yd^3 mixture

Field Mix Adjusted For Size	Weight (lb)	Volume (yd^3)
Cement	131.8	0.025
Sand	252.5	0.057
Rock	349.1	0.080
Water	61.8	0.037
Air	0	0.013
Admixtures		
mL HRWR for each batch=	109.04	mL
mL AEA Soln. for each batch=	36.35	mL
Water- wt. of admix.=	61.5	

Table 2 – Concrete compressive strength

Slab Side	28-day strength (psi) average
1	7940
2	7450

The experimental set up is shown in Figure 6, and includes a vertical servo-hydraulic actuator in-line with the pushout specimen. To vary the applied friction force at the steel-concrete interface, two steel plates are added to clamp the specimen slabs (see Figure 7) with controlled normal forces provided by instrumented threaded rods. Note that the specimen is placed on a grout bed prior to testing to provide uniform load transfer at the slab base (avoiding any load concentrations due to casting imperfections). Strain gauges are attached to each of the four threaded rods connecting the steel plates to measure the applied normal force. Figure 8 shows the steel clamping plate geometry, including stiffeners.

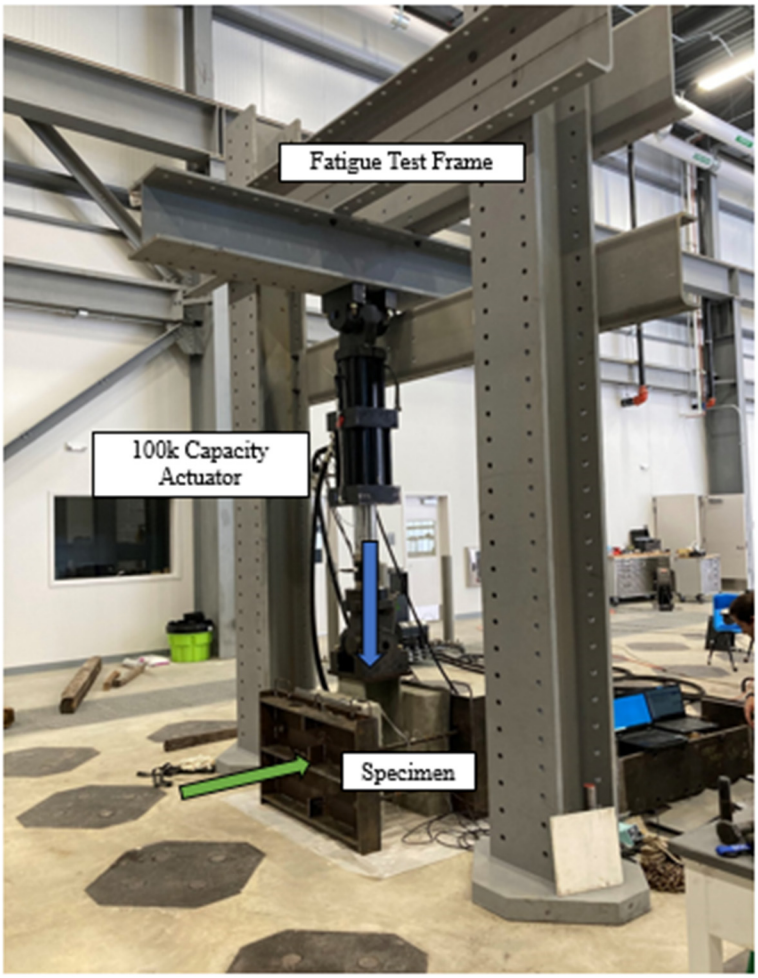

Figure 6 - Fatigue test frame setup

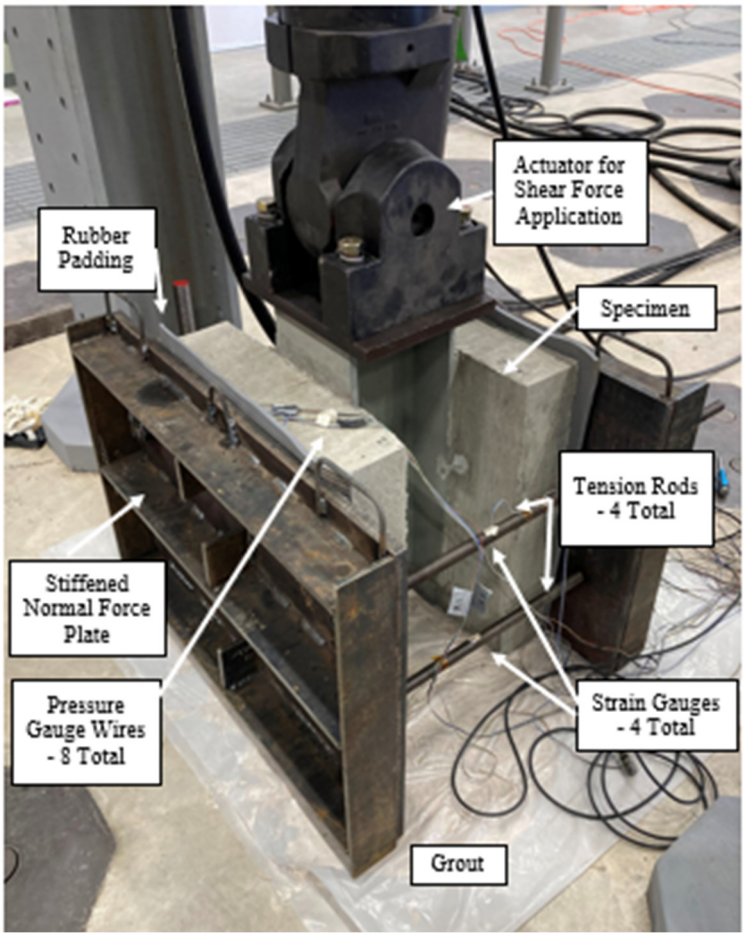

Figure 7 - Test setup detail

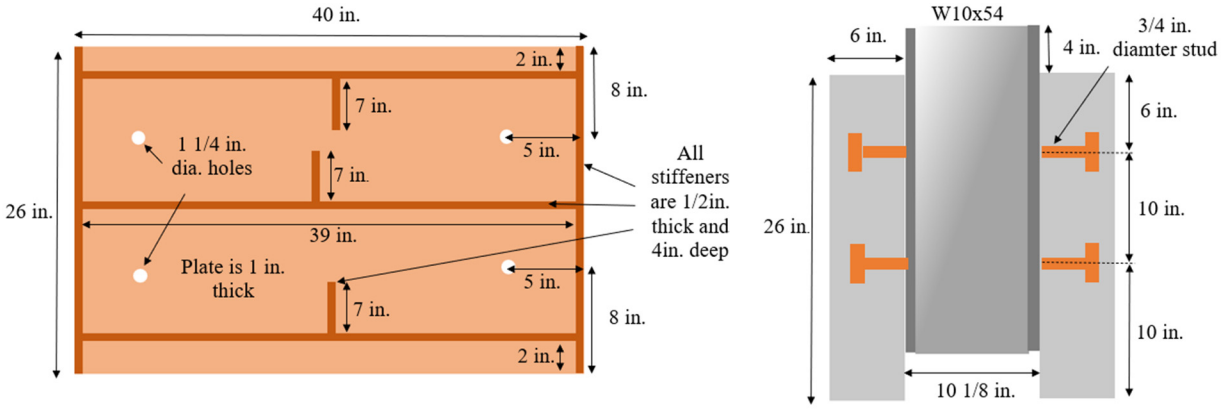

Figure 8 - Stiffened steel load plate and pushout specimen

2.1 Instrumentation and Loading

To directly measure forces transferred to the embedded studs, each stud in the IOZ coated specimen was instrumented with thin, transverse, foil pressure gauges (type PMS 40 manufactured by HBM, inc.). These pressure gauges are capable of measuring contact pressure between the concrete slab and steel stud. All pressure gauges were attached to the shear stud base (on the stud side expected to be in bearing) using Kapton tape as shown in Figure 9. PMS 40 pressure gauges record a change in resistance, which is calibrated to changes in pressure using Equation 1. Closed form elasticity equations related to rigid objects embedded within elastic materials were used by (Hillhouse & Prinz, 2020) to relate recorded pressures to applied forces as summarized below in Figure 10. A load cell in-line with the hydraulic actuator and pushout specimen measured applied loads to the specimen during testing, allowing direct comparison between load input and measured stud force.

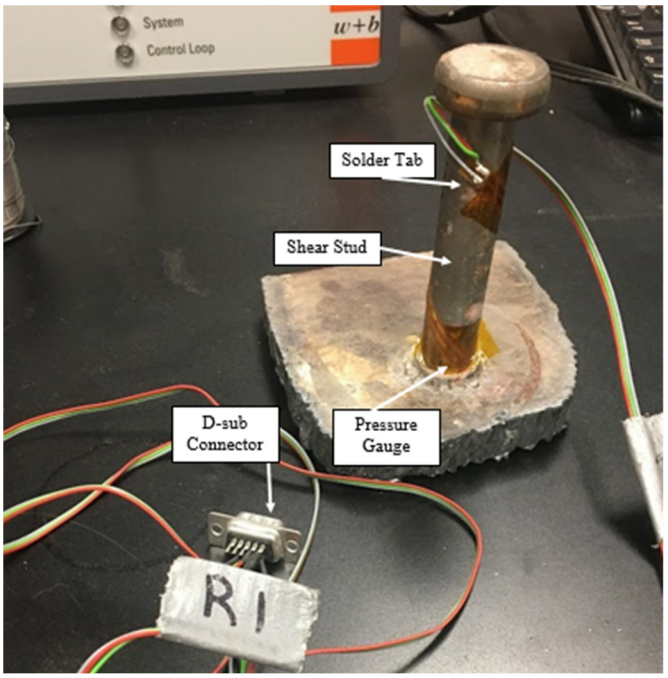

Figure 9 - Example shear stud instrumentation

$$\frac{\Delta R}{120\ \Omega} = 2.5\left(\frac{10^{-6}}{\text{bar}}\right) \times \Delta P \qquad \text{(Equation 1)}$$

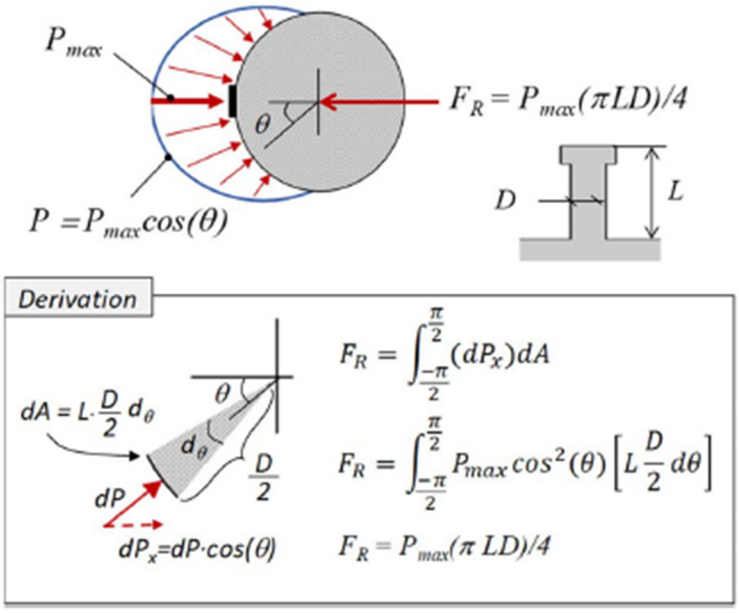

Figure 10 – Stud force from measured peak pressure (Hillhouse & Prinz, 2020)

Table 3 shows the loading protocol used to investigate friction effects on stud demands. In Table 3, three levels of normal force are applied to the slab (0k, 6.1k, and 10.1k) in combination with three levels of applied stud shear (an applied axial load in the test setup). At each normal force level, shear forces were applied over five constant amplitude cycles to ensure a steady state response. The chosen loading protocol results in nine separate test conditions for the IOZ specimen and allows direct comparison of stud demands between conditions having no friction, and those with increased friction levels.

Table 3 - Loading protocol

Specimen	Normal Force (k)	Shear Force (k) Per Normal Force	Cycles Per Force
IOZ	0	10, 15, 25	5
	6.1	10, 15, 25	
	10.1	10, 15, 25	

2.2 Coefficient of Static Friction Experiments

To allow friction load transfer estimations from the experiments, and to aid later analytical simulations (considering additional galvanized and cleaned mill-scale coatings) experiments were conducted to find the coefficient of friction between a rough concrete surface and IOZ, galvanized, and cleaned mill-scale surfaces. A simple inclined plane test setup (based on static equilibrium) was used to calculate the static coefficient of friction for each interface. Figure 11 shows the three girders used for the inclined plane sliding friction experiment. Figure 12 shows the free body diagram in equilibrium, wherein the coefficient of static friction is determined as the tangent of incline angle at sliding.

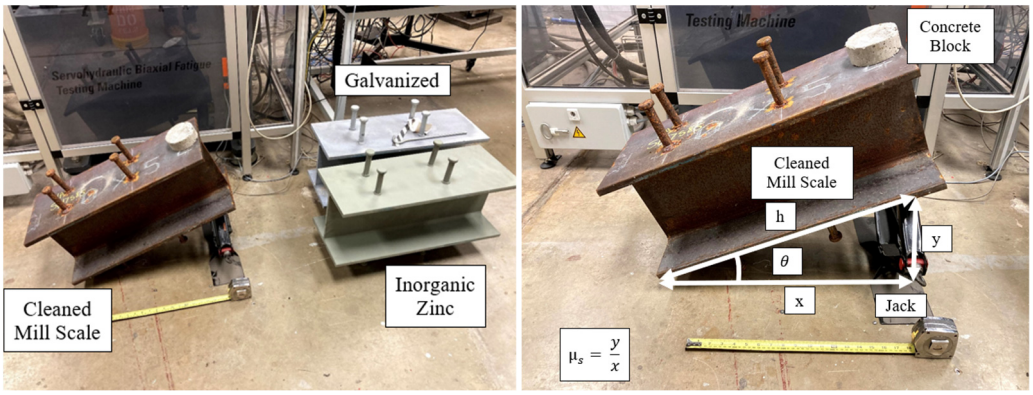

Figure 11 - Three steel coating types and inclined static friction test

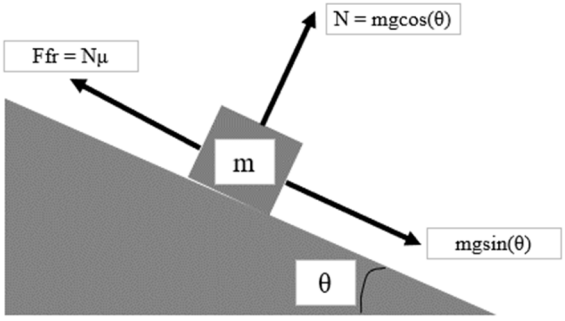

$\Sigma Fx = mg\sin(\theta) - N\mu = 0$
$= mg\sin(\theta) - mg\cos(\theta)\mu = 0$
$\mu = \sin(\theta)/\cos(\theta)$
$\mu = \tan(\theta) = y/x$

Figure 12 - Free body diagram of inclined static friction test

Table 4 shows the resulting friction coefficients from the inclined plane experiments. Three inclined plane experiments were completed for each coating type and the averages were calculated. In Table 4, the clean mill-scale surface had the lowest coefficient of 0.54 with galvanized and IOZ coatings providing increased friction at coefficients of 0.69 and 0.86 respectively.

Table 4 - Friction coefficients per coating type

Steel Coating Type	Friction Coefficient
Cleaned mill scale	0.54
Galvanized	0.69
Inorganic zinc	0.86

2.3 Results

Prior to the cyclic testing, an initial overload of 100k was applied to the specimen to break any adhesion bond between the steel surface and concrete slab, leaving all results as stud reactions and friction forces. Figure 14 shows the measured forces transferred through each stud during the 25k applied load cycles, at each level of applied normal force (0k, 6k, and 10k). In Figure 14, moderate normal force levels (6k) resulted in more than 60% decrease in stud demand, with 10k normal force providing 79% reduction on average. Visually, the 60% and 79% stud reaction decreases can be seen in the bar chart on the upper left-hand side of Figure 13. The black bars show the 0k normal force stud reactions, the medium gray bars show the 6k normal stud reactions, and the light gray bars show the 10k normal force stud reactions. Stud reactions for the 25k shear force for each normal force are higher than stud reactions under lower shear forces at 15k and 10k. Two pressure sensors were damaged in the process of fabricating the specimen and did not measure any resistance. The 6 graphs show the stud reactions per cycle under each shear load at 5 cycles per load and a decrease can be seen among the 0k, 6k, and 10k

applied normal forces. No normal forces greater than 10k were applied because stud reaction forces were very low and difficult to detect the 5 cycles.

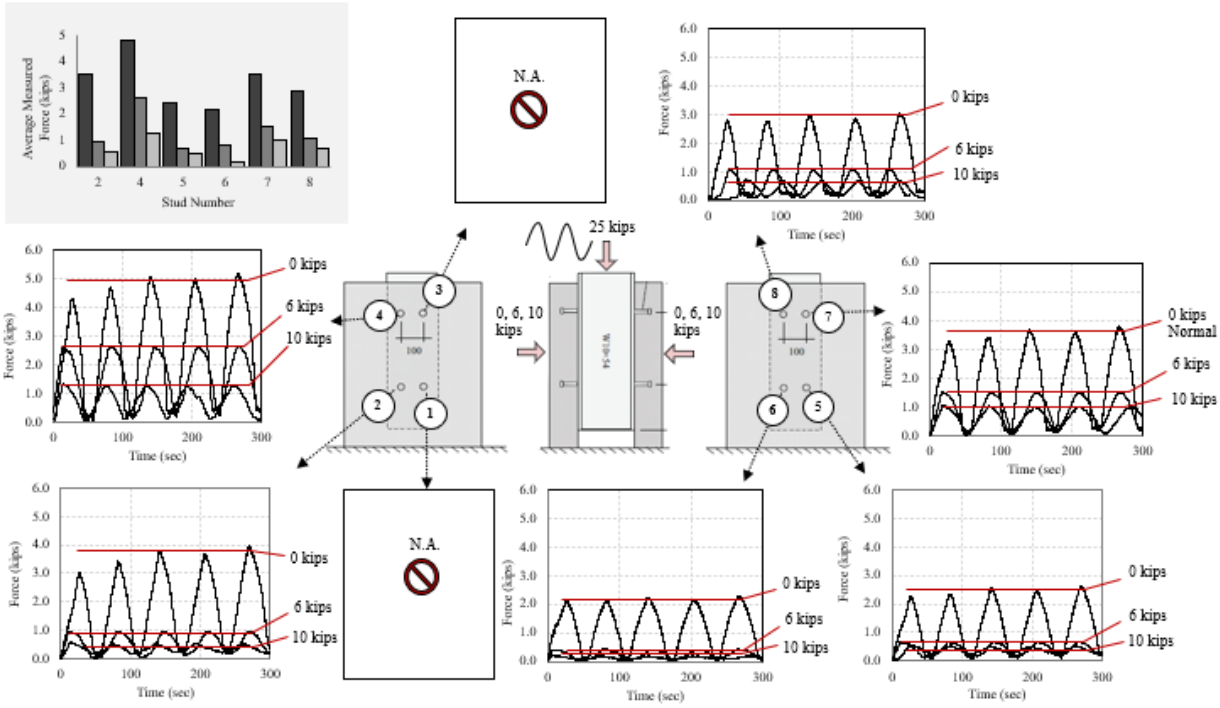

Figure 13 - 25k shear force stud reactions

Figure 14 shows lower applied loads (15k cycles) forces reduced stud demands by 74% at a normal force of 6k. Stud demands were reduced by 86% under the 10k normal force in Figure 14. At lower applied loads (10k cycles) applied friction through the 6k normal force reduced stud demands by over 85%, virtually eliminating the demands on the shear studs. Figure 15 shows the measured stud forces at 0k, 6k, and 10k normal force during the 10k applied cycles. In Figure 15, a noticeable decrease in measured stud force is seen once normal force is provided to the concrete slabs. Shear cycles lower than 10k were not used in the study as stud reactions were too low to detect all 5 shear cycles.

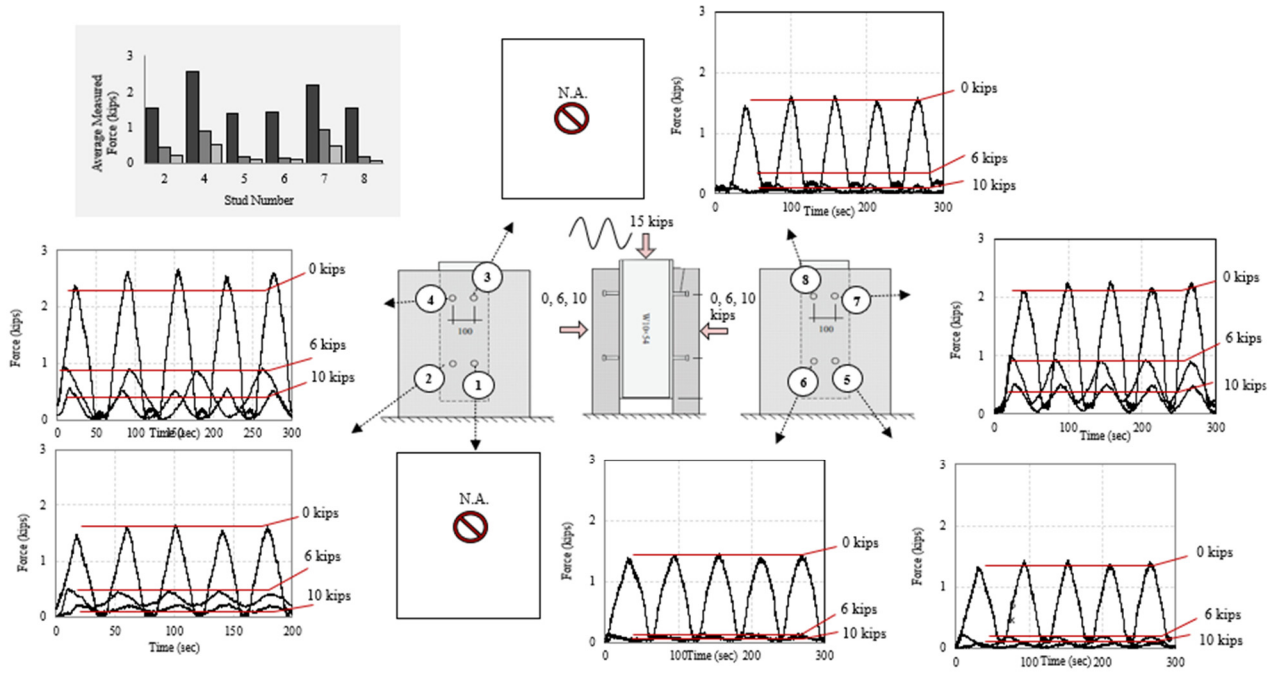

(b)

Figure 14 – 15k shear load stud reactions

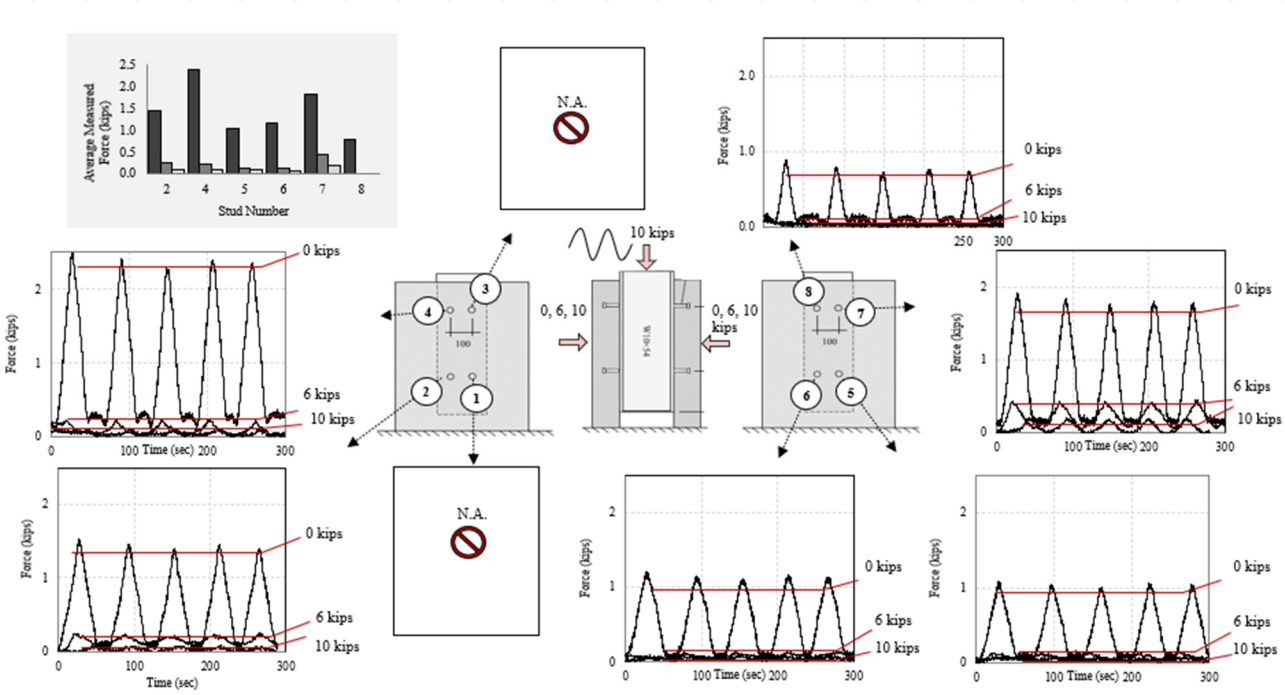

Figure 15 – 10k shear load stud reactions

Figure 16 shows increasing cumulative friction forces with increasing slab normal forces. The cumulative friction forces are based off six of the eight studs, as two of the pressure gauges were damaged during casting. At a 25k applied shear with 10k normal force, the friction force for six studs is nearly 20k indicating nearly all of the applied shear load is transferred through an alternative load path around the studs. The same friction pattern is seen for the 15k and 10k shear loads at a 10k normal force.

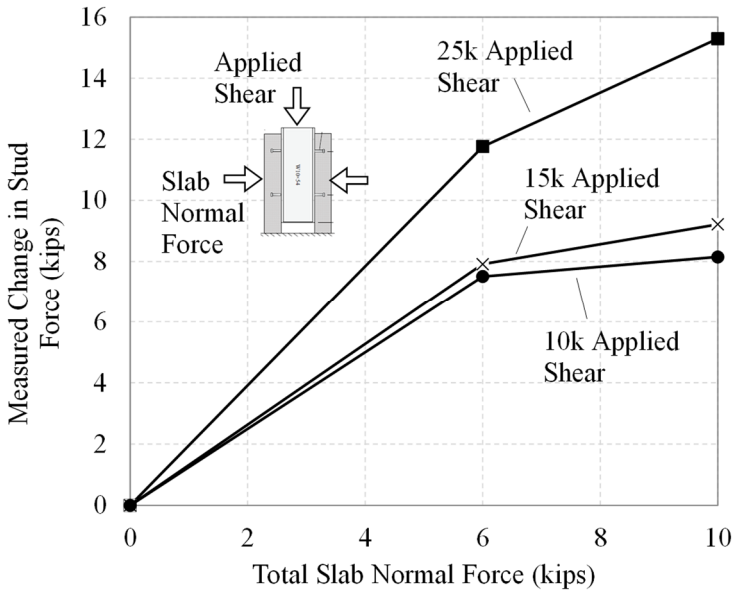

Figure 16 – Inorganic zinc friction forces

Table 5 shows the friction forces taken as percentage reductions per normal force. For the 6k normal force, the stud reductions are 60%, 74%, and 87% for the 25k, 15k, and 10k shear loads respectively. For the 10k normal force, the increased stud reductions are 78%, 86%, and 94% for the 25k, 15k, and 10k shear loads respectively. Increasing the normal force significantly increases the friction force reductions on the specimen.

Table 5 - Stud force reductions due to applied normal force

Applied Shear Force (k)	Applied Normal Force (k)	Cumulative stud force (k)	Stud force reduction (%)
25	0	19.4	0.0
	6	7.6	60.6
	10	4.1	78.8
15	0	10.7	0.0
	6	2.8	74.2
	10	1.4	86.4
10	0	8.6	0.0
	6	1.1	87.1
	10	0.5	94.6

3. Analytical Investigation

An analytical model of the pushout test performed was simulated using ABAQUS CAE to compare finite element friction results to the experimental data, and to compare steel treatment differences between inorganic zinc (IOZ) and clean mill scale (CMS) coated steel surfaces. Input values include the same calculated concrete Young's Modulus as the experimental specimens, friction penalties as recorded by the friction coefficient experiment, and equivalent normal and shear loads. All steel girder geometries were modeled using shell elements while the shear studs were simulated using wire/beam elements. All concrete slab geometries were simulated using solid elements such that the wire element studs could be embedded. Table 6 and Table 7 outline the various material input values for the steel and concrete elements, as well as the friction penalties considered based on the various surface coatings (IOZ and CMS). Figure 16 and Figure 17 show the model steel components and assembled steel-concrete complete model.

Table 6 - ABAQUS Young's modulus and Poisson's ratio inputs

Material	Young's Modulus, E (ksi)	Poisson's Ratio
Concrete	4475	0.2
Steel	29,000	0.3

Table 7 - ABAQUS coating input

Steel Coating Type	Friction Coefficient
Clean Mill Scale	0.54
Inorganic Zinc	0.86

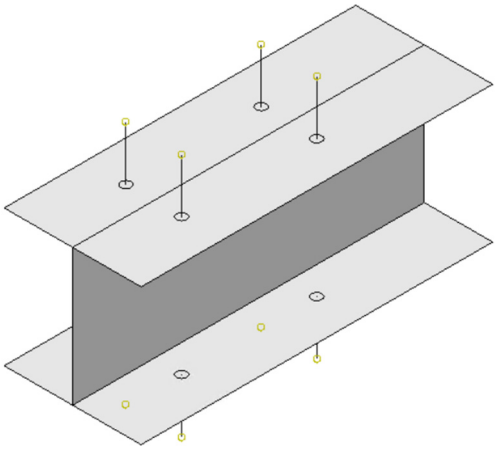

Figure 17 - ABAQUS shell model girder

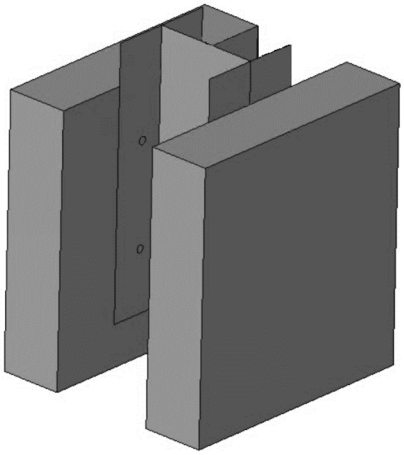

Figure 18 - ABAQUS pushout simulation

3.1 Analytical Inorganic Zinc and Cleaned Mill Scale Results

A total of 32 ABAQUS jobs were completed. Four normal forces were applied of (0k, 5k, 10k and 25k) with 5 cycles of shear forces (10k, 15k, 20k, and 25k) per normal force per specimen coating type (IOZ and CMS). The normal forces were applied as pressures in the program, to simulate truck wheel pressures exerted on the concrete decking. The pressures are 40psi, 16psi, 8psi, and 0psi for the 25k, 10k, 5k, and 0k normal forces respectively. Table 8 shows the results for each stud per loading case. The first sixteen tests report the IOZ specimen results and the second sixteen tests report the CMS specimen results. Job 1 and Job 17 were both run with 25k shear cycles and 25k normal force with friction coefficients as the only different between the two jobs. The IOZ cumulative stud forces were 3.36k and the CMS cumulative stud

forces were 0.5k higher at 3.88k. A higher friction coating like IOZ increases the friction force reduction compared to the CMS specimen.

Table 8 - ABAQUS IOZ and CMS Specimen Results

ABAQUS Model Inputs						max stud force (kips) stud number								
Job Number	Job Title	Coating	Axial Force (k)	Normal Force (k)	Normal (psi)	1	2	3	4	5	6	7	8	sum
1	25AINO40	0.86	25	25	40.1	0.46	0.46	0.35	0.46	0.46	0.35	0.35	0.46	3.3590
2	25AINO16	0.86	25	10	16.0	0.60	0.48	0.48	0.60	0.60	0.48	0.48	0.60	4.3366
3	25AINO08	0.86	25	5	8.0	0.67	0.55	0.55	0.68	0.68	0.55	0.55	0.67	4.8989
4	25AINO00	0.86	25	0	0.0	0.76	0.63	0.63	0.76	0.76	0.63	0.63	0.76	5.5541
5	20AINO40	0.86	20	25	40.1	0.37	0.28	0.28	0.37	0.37	0.28	0.28	0.37	2.6005
6	20AINO16	0.86	20	10	16.0	0.49	0.39	0.39	0.49	0.49	0.39	0.39	0.49	3.5010
7	20AINO08	0.86	20	5	8.0	0.55	0.44	0.44	0.55	0.55	0.44	0.44	0.55	3.9691
8	20AINO00	0.86	20	0	0.0	0.62	0.51	0.51	0.62	0.62	0.51	0.51	0.62	4.5334
9	15AINO40	0.86	15	25	40.1	0.28	0.20	0.20	0.28	0.28	0.20	0.20	0.28	1.9420
10	15AINO16	0.86	15	10	16.0	0.37	0.29	0.29	0.37	0.37	0.29	0.29	0.37	2.6489
11	15AINO08	0.86	15	5	8.0	0.42	0.33	0.33	0.42	0.42	0.33	0.33	0.42	3.0181
12	15AINO00	0.86	15	0	0.0	0.48	0.39	0.39	0.48	0.48	0.39	0.39	0.48	3.4747
13	10AINO40	0.86	10	25	40.1	0.19	0.12	0.12	0.19	0.19	0.12	0.12	0.19	1.2754
14	10AINO16	0.86	10	10	16.0	0.25	0.19	0.19	0.25	0.25	0.19	0.19	0.25	1.7798
15	10AINO08	0.86	10	5	8.0	0.29	0.22	0.22	0.29	0.29	0.22	0.22	0.29	2.0409
16	10AINO00	0.86	10	0	0.0	0.33	0.26	0.27	0.33	0.33	0.27	0.26	0.33	2.3716
17	25APMS40	0.54	25	25	40.1	0.55	0.42	0.42	0.55	0.55	0.42	0.42	0.55	3.8774
18	25APMS16	0.54	25	10	16.0	0.68	0.54	0.54	0.68	0.68	0.54	0.54	0.68	4.8491
19	25APMS08	0.54	25	5	8.0	0.73	0.59	0.59	0.73	0.73	0.59	0.59	0.73	5.2934
20	25APMS00	0.54	25	0	0.0	0.79	0.65	0.65	0.80	0.80	0.65	0.65	0.79	5.7740
21	20APMS40	0.54	20	25	40.1	0.45	0.33	0.33	0.45	0.45	0.33	0.33	0.45	3.1059
22	20APMS16	0.54	20	10	16.0	0.55	0.43	0.43	0.55	0.55	0.43	0.43	0.55	3.9101
23	20APMS08	0.54	20	5	8.0	0.59	0.47	0.47	0.60	0.60	0.47	0.47	0.59	4.2777
24	20APMS00	0.54	20	0	0.0	0.65	0.52	0.52	0.65	0.65	0.52	0.52	0.65	4.6854
25	15APMS40	0.54	15	25	40.1	0.34	0.24	0.24	0.34	0.34	0.24	0.24	0.34	2.3261
26	15APMS16	0.54	15	10	16.0	0.42	0.32	0.32	0.42	0.42	0.32	0.32	0.42	2.9543
27	15APMS08	0.54	15	5	8.0	0.45	0.36	0.36	0.45	0.45	0.36	0.36	0.45	3.2425
28	15APMS00	0.54	15	0	0.0	0.49	0.40	0.40	0.49	0.49	0.40	0.40	0.49	3.5676
29	10APMS40	0.54	10	25	40.1	0.23	0.15	0.15	0.23	0.23	0.15	0.15	0.23	1.5377
30	10APMS16	0.54	10	10	16.0	0.28	0.21	0.21	0.28	0.28	0.21	0.21	0.28	1.9826
31	10APMS08	0.54	10	5	8.0	0.31	0.24	0.24	0.31	0.31	0.24	0.24	0.31	2.1850
32	10APMS00	0.54	10	0	0.0	0.33	0.27	0.27	0.34	0.34	0.27	0.27	0.33	2.4164

Figure 19 and Figure 20 show the friction forces per normal force for IOZ and CMS specimens. The friction forces in Figures 19 and 20 are significantly less than corresponding friction forces in Figure 16. The IOZ specimen in Figure 19 exhibited higher friction load results (about 2.2k) compared to the CMS specimen in Figure 20 of about 1.9k.

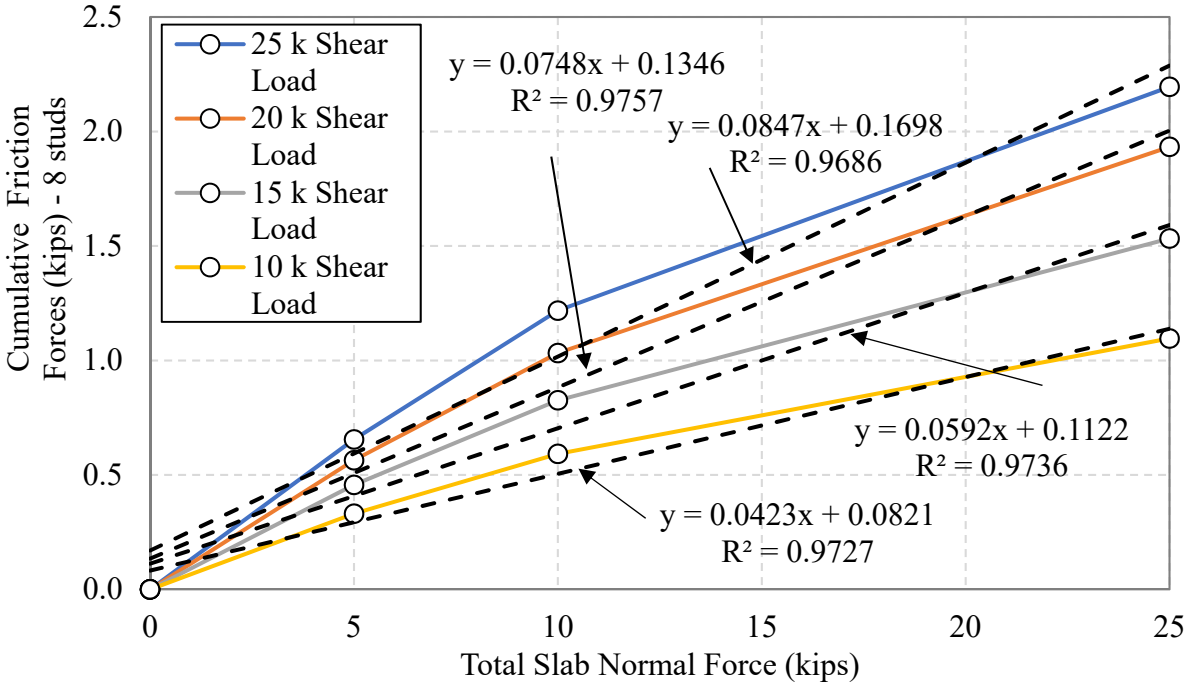

Figure 19 - IOZ analytical results - cumulative forces/normal force

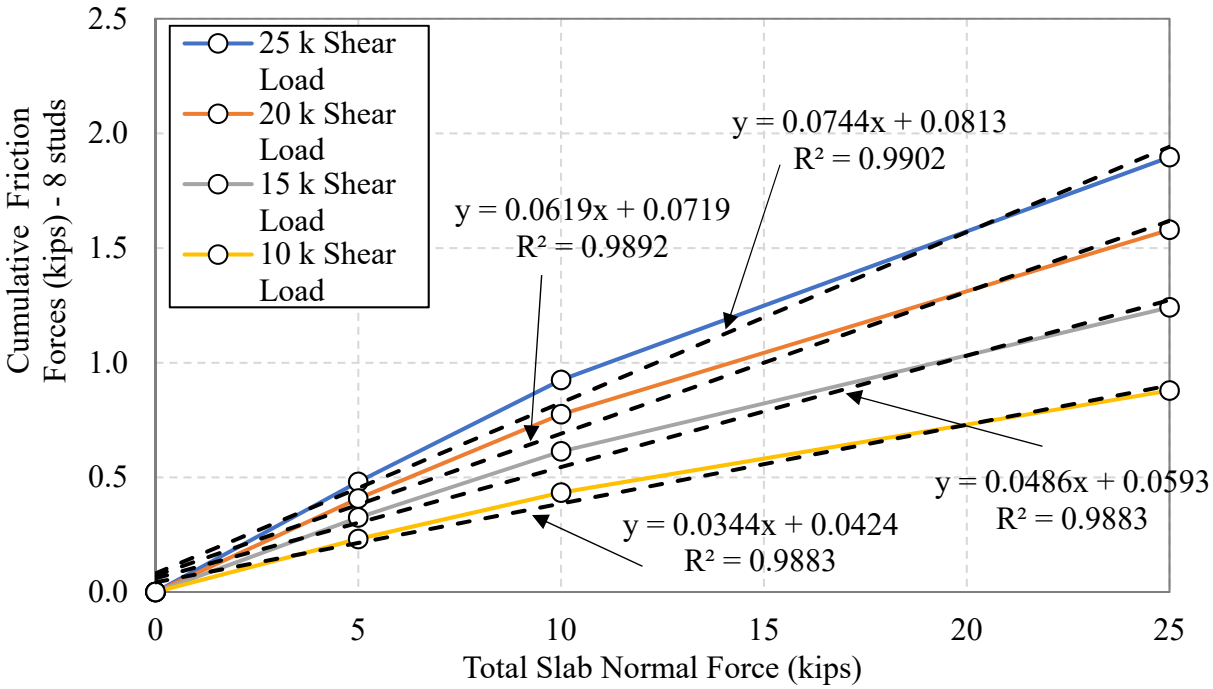

Figure 20 - CMS analytical results - cumulative forces/normal force

Figure 21 and Figure 22 show the stud forces per stud per normal force per shear load. In each case, the 0k normal force provided the greatest stud reactions, which was expected, as friction between the slab and steel flange would be lowest under this condition. The 25k normal force resulted in the lowest measured stud reactions for each shear load cycle.

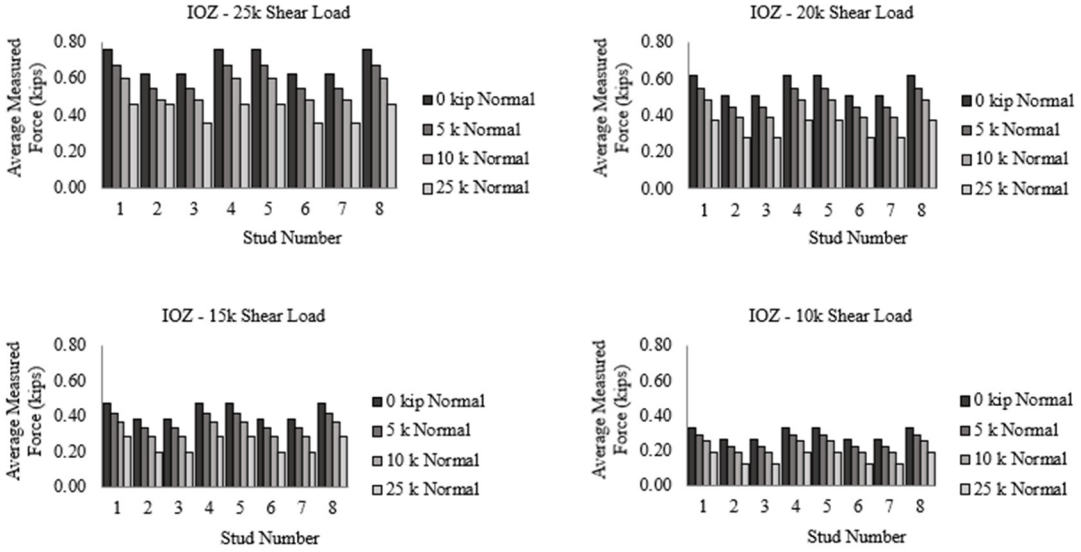

Figure 21 - IOZ - individual stud reactions per normal force and shear load

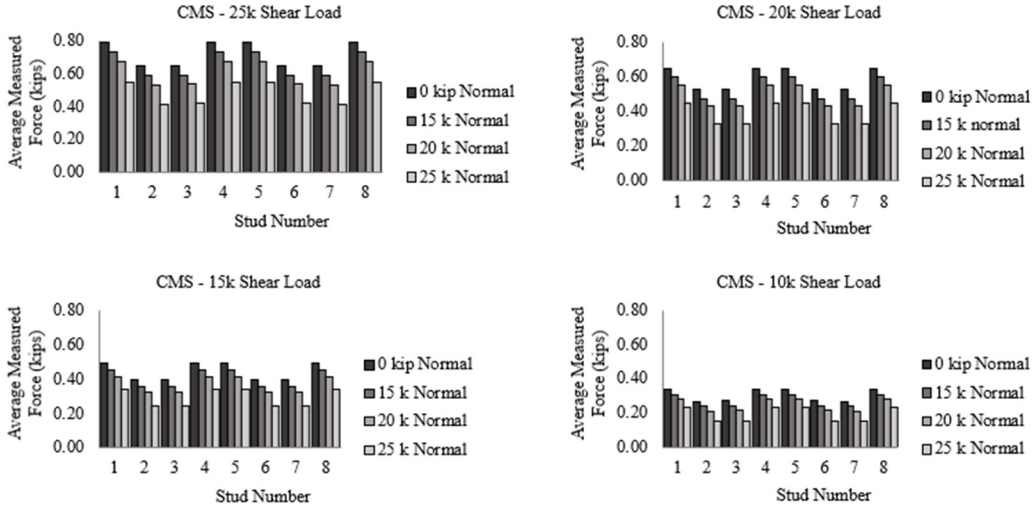

Figure 22 - CMS - individual stud reactions per normal force and shear load

Table 9 and Table 10 shows the friction force reduction taken as percentages for the IOZ and CMS specimens respectively. The greatest stud force reduction for the IOZ specimen is at 46.2% under the 10k shear load and 25k normal force shown in Table 9. The greatest stud force reduction for the CMS specimen is 36.4% also under the 10k shear load and 25k normal force shown in Table 10. There is a difference of almost 10% friction force reduction between the two cases as a results of the more rough IOZ coating having a greater friction coefficient. Again, increased normal forces increase the work done by friction as well as coating types better than CMS.

Table 9 - IOZ Analytical - Total Friction by %

Applied Shear (k)	Applied Normal Force (k)	Cumulative Stud Force (k)	Stud Force Reduction (%)
25	0	5.55	0.0
	5	4.90	11.8
	10	4.34	21.9
	25	3.36	39.5
20	0	4.53	0.0
	5	3.97	12.4
	10	3.50	22.8
	25	2.60	42.6
15	0	3.47	0.0
	5	3.02	13.1
	10	2.65	23.8
	25	1.94	44.1
10	0	2.37	0.0
	5	2.04	13.9
	10	1.78	25.0
	25	1.28	46.2

Table 10 - CMS Analytical - Total Friction by %

Applied Shear (k)	Applied Normal Force (k)	Cumulative Stud Force (k)	Stud Force Reduction (%)
	0	5.77	0.0
	5	5.29	8.3
25	10	4.85	16.0
	25	3.88	32.8
	0	4.69	0.0
	5	4.28	8.7
20	10	3.91	16.5
	25	3.11	33.7
	0	3.57	0.0
	5	3.24	9.1
15	10	2.95	17.2
	25	2.33	34.8
	0	2.42	0.0
	5	2.19	9.6
10	10	1.98	18.0
	25	1.54	36.4

Table11 compares experimental and analytical data for 3 studs, with predictions from the ABAQUS simulations estimating approximately 1/3 the stud demand measured in experiment.

Table 11 – Experimental and analytical comparison of three studs

Force Per Stud (k) - 0k Normal Force				
Shear (k)	Stud	Experimental	Analytical	
		IOZ	IOZ	CMS
25	4	4.80	0.76	0.80
	5	2.44	0.76	0.80
	6	2.19	0.63	0.65
15	4	2.56	0.48	0.49
	5	1.39	0.48	0.49
	6	1.41	0.39	0.40
10	4	2.38	0.33	0.34
	5	1.04	0.33	0.34
	6	1.15	0.27	0.27

4. Conclusions and Recommendations

In this study, the effects of flange surface friction on load transfer in composite girders was investigated experimentally through double-sided pushout testing and analytically through detailed finite element analysis. A total of 9 pushout tests were conducted on inorganic zinc primer coated steel flanges to quantify stud demand reductions due to friction. A total of 32 finite element analyses investigated flange surface effects of other common flange coatings. The following conclusions and recommendations result from the experimental and analytical study.

1) Moderate levels of applied normal force (6k) to the concrete slab result in large (greater than 60% on average) reductions in stud demands due to friction load transfer bypassing the embedded studs. At lower levels of applied shear (10 kips), friction effects due to applied slab normal force almost completely eliminated demands on the studs (a 94.6% reduction in stud demand occurred under 10 kip normal force).
2) While ultimately dependent on the applied normal force, the proposed 0.5 friction demand reduction value proposed by Hillhouse and Prinz (Hillhouse & Prinz, 2020) appears reasonable.
3) Analytical and experimental measurements demonstrate non-uniform stud demand distributions in the vertically loaded double-sided pushout configuration, which may have implications for interpreting “failure” in previous fatigue capacity studies wherein stud shear stress ranges are assumed to be uniform.

Recommended Modifications for Future work

It would be advisable for future tests, to adjust the loading setup. This study applied the normal force by tightening four tensions rods connecting two pressure plates. It was difficult to

set the normal force using the strain gauges. It is suggested to use a horizontal actuator to apply the normal force and allow the normal force to be targeted better.

5. References

AASHTO, "AASHTO LRFD bridge design specifications (9th edition)," American Association of State Highway and Transportation Officials, 2020.

Berthet, J. F., Yurtdas, I., Delmas, Y., & Li, A. (2011). Evaluation of the adhesion resistance between steel and concrete by push out test. *International Journal of Adhesion and Adhesives*, *31*(2), 75–83. https://doi.org/10.1016/j.ijadhadh.2010.11.004

Gattesco, N., Giuriani, E., Gubana, A., Low-Cycle fatigue Test on Shear Connectors. (1997). *123*(FEBRUARY), 145–150.

Hillhouse, B., & Prinz, G. S. (2020). Effects of Clustering and Flange Surface Friction on Headed Shear Stud Demands. *Journal of Bridge Engineering*, *25*(6), 04020026. https://doi.org/10.1061/(asce)be.1943-5592.0001562

Huo, J., Wang, H., Zhu, Z., Liu, Y., & Zhong, Q. (2018). Experimental Study on Impact Behavior of Stud Shear Connectors between Concrete Slab and Steel Beam. *Journal of Structural Engineering*, *144*(2), 04017203. https://doi.org/10.1061/(asce)st.1943-541x.0001945

Kakish, H. F., Splittgerber, D. L., Baishya, M. C., & Tadros, M. K. (1999). Large studs for composite action in steel bridge girders. *Transportation Research Record*, *7*(1688), 53–61. https://doi.org/10.3141/1688-07

Lee, K.-C., Abbas, H. H., & Ramey, G. E. (2010). *Review of Current AASHTO Fatigue Design Specifications for Stud Shear Connectors*.

Lin, J. P., Wu, Z. B., Yin, Y., & Feng, F. (2020). Analysis of Shear Connector of Steel–Concrete Composite Box-Girder Bridge Considering Interfacial Bonding and Friction. *International Journal of Steel Structures*, *20*(2), 452–463. https://doi.org/10.1007/s13296-019-00296-2

Luo, Y., Hoki, K., Hayashi, K., & Nakashima, M. (2016). Behavior and Strength of Headed Stud–SFRCC Shear Connection. I: Experimental Study. *Journal of Structural Engineering*, *142*(2), 04015112. https://doi.org/10.1061/(asce)st.1943-541x.0001363

Ovuoba, B., & Prinz, G. S. (2016). Fatigue Capacity of Headed Shear Studs in Composite Bridge Girders. *Journal of Bridge Engineering*, *21*(12), 04016094. https://doi.org/10.1061/(asce)be.1943-5592.0000915

Ovuoba, B., & Prinz, G. S. (2018a). Headed Shear Stud Fatigue Demands in Composite Bridge Girders Having Varied Stud Pitch, Girder Depth, and Span Length. *Journal of Bridge Engineering*, *23*(11), 04018085. https://doi.org/10.1061/(asce)be.1943-5592.0001303

Ovuoba, B., & Prinz, G. S. (2018b). Investigation of residual fatigue life in shear studs of existing composite bridge girders following decades of traffic loading. *Engineering Structures*, *161*(February), 134–145. https://doi.org/10.1016/j.engstruct.2018.02.018

Sjaarda, M., Porter, T., West, J. S., & Walbridge, S. (2017). Fatigue Behavior of Welded Shear Studs in Precast Composite Beams. *Journal of Bridge Engineering*, *22*(11), 04017089. https://doi.org/10.1061/(asce)be.1943-5592.0001134

Slutter, R. G., & Fisher, J. W. (1966). Fatigue Strength of Shear Connectors. *45th Annual Meeting of the Highway Research Board, 315(147).* http://trid.trb.org/view.aspx?id=1306976

Veljkovic, M., Johansson, B., (2006). Residual Static Resistance of Welded Stud Shear Connectors. *Proceedins of the 5th International Conference on Composite Construction in Steel and Concrete V (2006), 10.4061/40826(186)49*

Xia, Y., Chen, L., Ma, H., & Su, D. (2019). Experimental and numerical study on shear studs connecting steel girder and precast concrete deck. *Structural Engineering and Mechanics*, *71*(4), 433–444. https://doi.org/10.12989/sem.2019.71.4.433

Xu, C., Sugiura, K., & Su, Q. (2018). Fatigue Behavior of the Group Stud Shear Connectors in Steel-Concrete Composite Bridges. *Journal of Bridge Engineering*, *23*(8), 04018055. https://doi.org/10.1061/(asce)be.1943-5592.0001261

Xue, W., Ding, M., Wang, H., & Luo, Z. (2008). Static Behavior and Theoretical Model of Stud Shear Connectors. *Journal of Bridge Engineering*, *13*(6), 623–634. https://doi.org/10.1061/(asce)1084-0702(2008)13:6(623)